

Nanostructure formation process in low-fluence femtosecond-laser ablation of thin film surface

Godai Miyaji and Kenzo Miyazaki

Institute of Advanced Energy, Kyoto University, Kyoto 611-0011, Japan

We have performed a pump and probe experiment for real-time reflectivity measurements as a function of superimposed laser shots at the fluence below the ablation threshold to induce nanostructure formation on thin films of diamond-like carbon (DLC). The evolution of reflectivity resolved the bonding structure change and the nanostructure formation through coherent interaction between the probe pulse and the film surface excited with the pump pulse. The characteristic reflectivity changes observed show that the nanostructure formation is preceded by the bonding structure change to swell the film surface. Based on the experimental results, we discuss the ultrafast dynamics of the nanostructure formation.

OCIS codes: 140.3390, 310.1860, 320.7160.

In the recent experiments of femtosecond (fs) laser ablation, Yasumaru *et al.* have found that superimposed laser pulses at low fluences produce periodic nanostructures with the spacing as small as $1/10 - 1/5$ of the laser wavelength on the hard thin films such as TiN and diamond-like carbon (DLC)^[1,2]. In addition, they have also observed that the nanostructure formation on the DLC surface is accompanied by a selective and irreversible bonding structure change from DLC to glassy carbon (GC), while no thin film technology for the GC has been developed so far^[3,4]. These phenomena suggest a promising approach to new nano-scale processing and machining of materials. One of the most important subjects to study should be the physical process responsible for the nanostructure formation and the bonding structure change. For the purpose of understanding this process, Miyazaki *et al.* and the present authors have investigated the reflectivity change induced in the ablation of the DLC film surface, and have shown that this change is closely associated with the modification of DLC to provide a good measure to monitor the interaction process on the surface^[4,5].

In this paper, we report the in-situ reflectivity measurements in the fs-laser ablation of DLC film. A pump-probe technique has been used to study dynamic processes for the morphological and bonding structure changes on DLC.

The samples were 1.6- μm -thick DLC films deposited on polished Si substrates with a magnetron sputtering system. The laser used for irradiation was a chirped pulse amplification Ti:sapphire laser system, providing linearly polarized laser pulses of ~ 100 -fs duration at a center wavelength of 800 nm. In pump-probe experiment, the output was split into two beams to produce a pump and a probe pulse. The pump pulse for ablation was focused in air at normal incidence onto the DLC surface to a Gaussian spot diameter ($1/e^2$) of $\sim 230 \mu\text{m}$. The probe pulse was passed through a delay line with the time delay of $\Delta t = 0 - 70$ ps between the pump and probe pulses, and was focused at the angle of $\theta = 4^\circ$ to a spot diameter of $\sim 160 \mu\text{m}$ in the center of the region irradiated by the pump pulse to measure the reflectivity R . The pump fluence F (J/cm^2) on the target was evaluated from the pulse energy and the focal spot size, and was varied in a range of $F = 0.06 - 0.2 \text{ J}/\text{cm}^2$. The film surface was exposed to multiple pulses of $N = 0 - 1000$ shots to induce ablation at the laser fluence below the single-pulse ablation threshold of the DLC films. The probe pulse fluence was suppressed to $0.2 \times 10^{-3} \text{ J}/\text{cm}^2$, so that the probe pulse itself did not induce any modification of the DLC films. The reflectivity R was defined by the ratio of the incident probe pulse energy to the reflected energy at the surface measured with calibrated P-I-N silicon photodiodes. The detected probe signals were

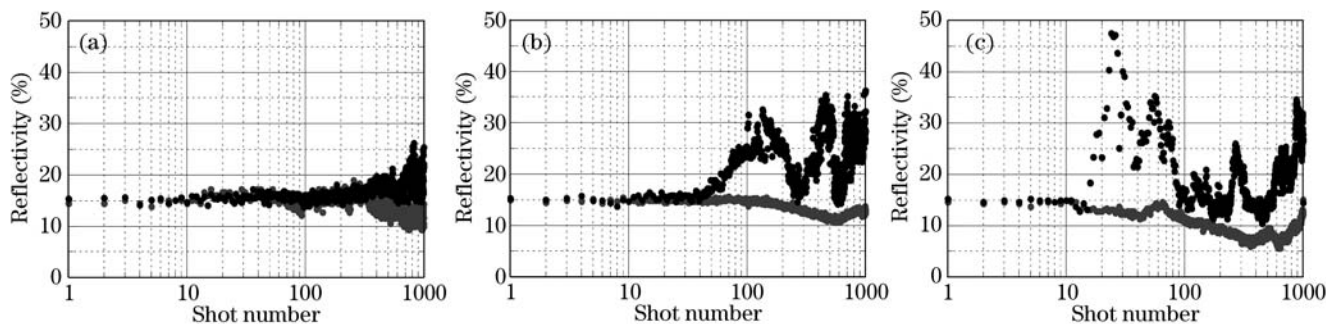


Fig. 1. Reflectivity measured with the probe pulses at $\Delta t = 0$ as a function of N for three different fluences. The pump and probe polarizations are parallel for the black circles and perpendicular for the gray circles. (a) $F = 0.11 \text{ J}/\text{cm}^2$, (b) $F = 0.14 \text{ J}/\text{cm}^2$, (c) $F = 0.17 \text{ J}/\text{cm}^2$.

recorded shot by shot with a personal computer through a fast analog-to-digital converter. The modification of the bonding structure was studied with Raman spectroscopy using a 514.5-nm argon ion laser beam of the 10- μm spot diameter focused onto the sample surface, which was efficient to provide a good signal to noise ratio of the spectrum without changing the bonding structure. The surface morphology of broad ($30 \times 30 \mu\text{m}$) and small ($1 \times 1 \mu\text{m}$) areas was observed with a scanning probe microscope (SPM).

Figure 1 shows the shot number evolution of the reflectivity changes measured at $\Delta t = 0$ for three different fluences of the pump pulses of which polarizations are parallel and perpendicular to the probe. It is noted in Fig. 1 that the reflectivity R increased when the laser shot number N increased for parallel polarizations (black circles), while R decreased monotonously for perpendicular polarizations (gray circles). We observed the enhancement of R in the region of $F = 0.11 - 0.18 \text{ J/cm}^2$. As seen in Figs. 1(b) and (c), R shows two peaks as N increases, and they are observed to appear at smaller N for larger F . The large peaks appear at $N \sim 140$ and 460 for $F = 0.14 \text{ J/cm}^2$, and at $N \sim 25$ and 50 for $F = 0.17 \text{ J/cm}^2$. For $F = 0.11 \text{ J/cm}^2$, we see the single large peak at $N \sim 700$, as shown in Fig. 1(a). In addition, such enhancement of the R was never observed at $\Delta t \geq 0.2 \text{ ps}$ even for parallel polarizations. These results suggest that the enhancement of R is certainly induced by coherent interaction between the probe pulse and the film surface excited with the pump pulse.

To study the coherent interaction in detail, we investigated the correlation between the change in the R and the DLC surface morphology with the SPM. Figure 2 shows the images of the DLC surface irradiated with $N = 0$ (a), 130 (b), 300 (c), 400 (d), and 500 (e) at $F = 0.14 \text{ J/cm}^2$. The initial surface roughness is $\sim 15 \text{ nm}$ in root-mean-square (rms) value estimated by the SPM image, as shown in Fig. 2(a). At $N = 130$, where the R increases to $\sim 33\%$ in Fig. 1(b), we see interference pattern formed due to swelling of the surface, as shown in the upper image of Fig. 2(b). The mean spacing between two peaks or crests of the fringe was measured to be $\sim 11 \mu\text{m}$, corresponding to $\lambda / \sin \theta$ at $\lambda = 800 \text{ nm}$ and $\theta = 4^\circ$. The lower image of Fig. 2(b) shows that no ablation to produce the nanostructure is induced on the fringe. In

the fs laser ablation experiments, such swelling of DLC surface has been observed to result from the mass density change, owing to the modification from DLC to GC or graphite^[6,7]. When the grating is formed on the surface, the pump pulse can partially be diffracted into the direction of the reflected probe beam to increase R . We could estimate the diffraction efficiency of $\sim 0.5\%$ for the surface shown in Fig. 2(b). This diffraction leads to an increase in R by $\sim 20\%$, which is in good agreement with $R \sim 33\%$, as shown in Fig. 1(b). At $N = 300$, where the R decreased down to $\sim 20\%$, the grating groove is observed to disappear on the surface, as shown in the upper image of Fig. 2(c), due to ablation initiated at the crest, while the periodic nanostructure of mean spacing 80 nm starts to be observed on the crest, as seen in the lower image of Fig. 2(c). With a further increase in N to 400, as shown in the upper image of Fig. 2(d), the ablation reverses the crest and trough of initial grating observed at $N = 130$, while the trough swells continuously due to incident pump field, and the R increases up to $\sim 35\%$. With $N = 500$, the deep nanostructure of the mean spacing $\sim 100 \text{ nm}$ is formed, as seen in the lower image of Fig. 2(e), where the second peak of R is observed, as shown in Fig. 1(b). In addition, the diffracted pump wave was also detected in the backward direction with respect to the incident probe pulse. These results demonstrate that the enhanced R in Fig. 1 is certainly due to the grating formation on the DLC surface.

To confirm the above discussion on the characteristic reflectivity R at $\Delta t = 0$, we observed the Raman spectra of the DLC surfaces. Figure 3 shows the spectra of the film surfaces irradiated with $N = 0$ (curve 1), 100 (curve 2), 300 (curve 3), and 500 (curve 4) of the pump pulse at $F = 0.14 \text{ J/cm}^2$. The spectrum of DLC shows a peak at the shift of 1530 cm^{-1} , as seen in curve 1 of Fig. 3, whereas the other three represent the typical spectra of GC that include two peaks at 1355 and 1590 cm^{-1} ^[3,4]. These spectra demonstrate that the structural change from DLC to GC is induced at $N \sim 100$ around the first peak of R plot seen in Fig. 1(b), where neither ablation nor nanostructure formation is induced yet, as shown in Fig. 2(b). This indicates that the change in bonding structure certainly precedes the nanostructure formation. Furthermore, comparing with the spectrum at $N = 100$,

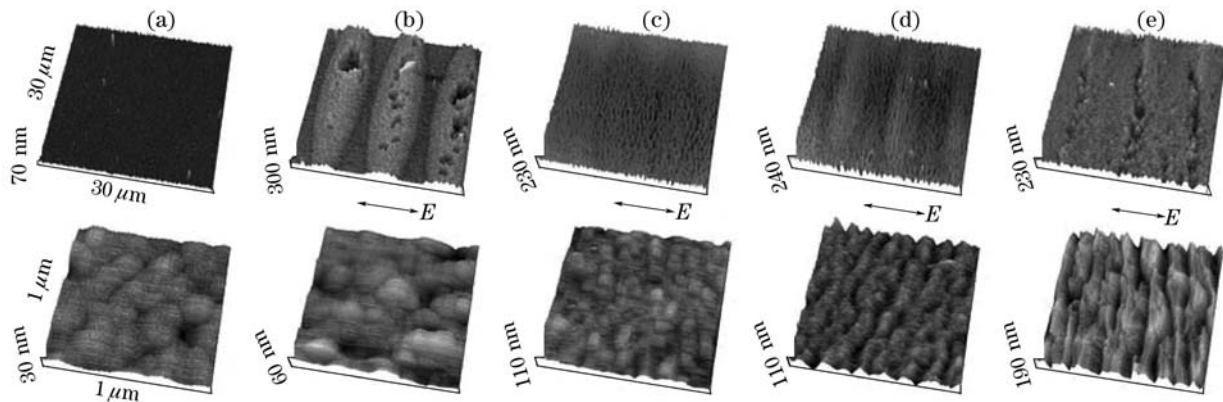


Fig. 2. Images of the DLC surface irradiated with (a) $N = 0$, (b) 130, (c) 300, (d) 400, and (e) 500 at $F = 0.14 \text{ J/cm}^2$ and $\Delta t = 0$ with the parallel polarizations. The upper images are for the central area of $30 \times 30 \mu\text{m}$ and the lower ones are for $1 \times 1 \mu\text{m}$ on the focal spot. The arrows represent the polarization direction.

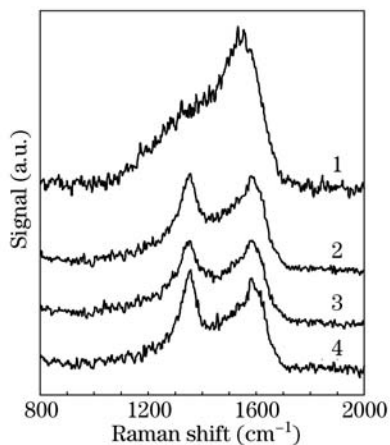


Fig. 3. Raman spectra of the DLC surfaces irradiated with $N = 0$ (curve 1), 100 (curve 2), 300 (curve 3) and 500 (curve 4) at $F = 0.14 \text{ J/cm}^2$ and $\Delta t = 0$ with the parallel polarizations.

we notice that the spectra at $N = 300$ and 500 include the smaller and larger peaks, respectively. This suggests that the fraction of GC slightly decreases at $N = 300$ where R is minimized and increases at $N = 500$ where R is peaked. These results show that the characteristic change of R is closely related to the morphological and bonding structure changes on the film surface.

Based on these results obtained, we propose the following process with respect to the nano-scale modification of the DLC surface. The structural change from DLC to GC corresponds to the transition of the sp^3 bond in DLC to the different stable structure of sp^2 for GC, which is due to the smaller dissociation energy of sp^3 bond than that of sp^2 [4]. As seen above, this change can be induced at the fluence F lower than the single-shot ablation threshold. With an increase in N , the incident laser pulse energy is partially stored in the thin film through the bonding structure change, and then the structural change is accumulated and detected as the surface swelling to form the grating at $N = 130$, as seen in Fig. 2(b). With a further increase in N , the GC layer starts to be ablated from the film surface to form the nanostructure, since the sp^2 bonds tend to preferentially be ionized with the fs laser pulses due to the lower ionization potential than that of sp^3 . Thus, the bonding structure change precedes the nanostructure formation or the ablation of thin film surface.

Although the results presented in the lower image of Fig. 2(c) show that the measurable nanostructure is formed at $N = 300$, the nano-scale ablation would start to locally be induced in a region of $N < \sim 300$. The decrease in R after the first peak suggests that this local ablation would preferentially take place in such small surface area that has contributed to the most efficient enhancement of R . In fact, the peaks in the GC spectra are weakened at $N \sim 300$, as seen in curve 3 of Fig. 3, sug-

gesting the partial removal of this area. With increasing N up to $N > 300$, the transitions from DLC to GC are grown again on the structured or ablated surface to result in the formation of the deep nanostructure at $N \sim 500$. These processes would be repeated with an increase in N until the DLC layer is completely removed from the surface.

The present experiment has also demonstrated that the small modulation of the pump field created by the weak probe pulse with a fluence of $\sim 1/700$ of the pump has produced a large morphological change or the grating formed through the accumulation of bonding structure change in the DLC films, as shown in the upper images of Fig. 2. This observation strongly suggests that weak local fields are generated to induce the nano-scale ablation and resulting nanostructure formation on the DLC surface[5]. We are making further experimental and theoretical studies to understand the detail of physical processes for the local field generation and resulting nanostructure formation.

In conclusion, using the pump and probe technique we have investigated the characteristic reflectivity changes in the nano-scale modification of the DLC films with fs laser pulses to understand the interaction dynamics for the modification from DLC to GC and the nanostructure formation. We have successfully resolved ultrafast evolution from the former to the latter through the characteristic enhancement of the reflectivity, owing to the selective change in the bonding structure from sp^3 to sp^2 to induce the swelling of the film surface. The experimental results demonstrate that the formation of periodic nanostructure is preceded by the change in the bonding structure of DLC, and suggest that the periodic nanostructure formation on the film surface is induced by the weak local field on the rough surface.

G. Miyaji's e-mail address is g-miyaji@iae.kyoto-u.ac.jp.

References

1. N. Yasumaru, K. Miyazaki, and J. Kiuchi, Appl. Phys. A **76**, 983 (2003).
2. N. Yasumaru, K. Miyazaki, and J. Kiuchi, Appl. Phys. A **81**, 933 (2005).
3. N. Yasumaru, K. Miyazaki, and J. Kiuchi, Appl. Phys. A **79**, 425 (2004).
4. K. Miyazaki, N. Maekawa, W. Kobayashi, M. Kaku, N. Yasumaru, and J. Kiuchi, Appl. Phys. A **80**, 17 (2005).
5. G. Miyaji and K. Miyazaki, Appl. Phys. Lett. **89**, 191902 (2006).
6. N. Yasumaru, K. Miyazaki, and J. Kiuchi, Appl. Phys. A **79**, 425 (2004).
7. T. V. Kononenko, V. V. Kononenko, S. M. Pimenov, E. V. Zavedeev, V. I. Konov, V. Romano, and G. Dumitru, Diamond Relat. Mater. **14**, 1368 (2005).